5426 *Biochemistry* **2010,** *49,* 5426–5435
DOI: 10.1021/bi100276b

BIOCHEMISTRY
including biophysical chemistry & molecular biology
Article

Chronic Cholesterol Depletion Using Statin Impairs the Function and Dynamics of Human Serotonin$_{1A}$ Receptors[†]

Sandeep Shrivastava, Thomas J. Pucadyil,[‡] Yamuna Devi Paila, Sourav Ganguly, and Amitabha Chattopadhyay*

Centre for Cellular and Molecular Biology, Council of Scientific and Industrial Research, Uppal Road, Hyderabad 500 007, India. [‡]Present address: Department of Cell Biology, The Scripps Research Institute, La Jolla, CA 92037.

Received February 24, 2010; Revised Manuscript Received May 12, 2010

ABSTRACT: Statins are potent inhibitors of HMG-CoA reductase, the key rate-limiting enzyme in cholesterol biosynthesis, and are some of the best selling drugs globally. We have explored the effect of chronic cholesterol depletion induced by mevastatin on the function of human serotonin$_{1A}$ receptors expressed in CHO cells. An advantage with statins is that cholesterol depletion is chronic which mimics physiological conditions. Our results show a significant reduction in the level of specific ligand binding and G-protein coupling to serotonin$_{1A}$ receptors upon chronic cholesterol depletion, although the membrane receptor level is not reduced at all. Interestingly, replenishment of mevastatin-treated cells with cholesterol resulted in the recovery of specific ligand binding and G-protein coupling. Treatment of cells expressing serotonin$_{1A}$ receptors with mevastatin led to a decrease in the diffusion coefficient and an increase in the mobile fraction of the receptor, as determined by fluorescence recovery after photobleaching measurements. To the best of our knowledge, these results constitute the first report describing the effect of chronic cholesterol depletion on the organization and function of a G-protein-coupled neuronal receptor. Our results assume significance in view of recent reports highlighting the symptoms of anxiety and depression in humans upon statin administration, and the role of serotonin$_{1A}$ receptors in anxiety and depression.

Cholesterol is an essential and representative lipid in higher eukaryotic cellular membranes and is crucial in membrane organization, dynamics, function, and sorting (*1*, *2*). It is often found distributed nonrandomly in domains in biological and model membranes (*3*, *4*). Many of these domains (sometimes termed "lipid rafts") are believed to be important for the maintenance of membrane structure and function. The idea of such specialized membrane domains assumes significance in cellular physiology since important functions such as membrane sorting and trafficking (*5*), signal transduction processes (*6*), and the entry of pathogens (*7*, *8*) have been attributed to these domains. Importantly, cholesterol plays a vital role in the function and organization of membrane proteins and receptors (*9*−*11*).

Cholesterol is the end product of a long and multistep sterol biosynthetic pathway that parallels sterol evolution (*12*). Statins are competitive inhibitors of HMG-CoA reductase,[1] the key enzyme in cholesterol biosynthesis that catalyzes the rate-limiting step in the biosynthetic pathway. This specific step involves the conversion of HMG-CoA into mevalonate, the precursor of cholesterol and other isoprenoids. Statins represent some of the best selling drugs globally and in clinical history. They are extensively used as oral cholesterol lowering drugs to treat hypercholesterolemia and dyslipidemia (*13*, *14*).

The G-protein-coupled receptor (GPCR) superfamily is the largest and most diverse protein family in mammals, involved in signal transduction across membranes (*15*, *16*). The serotonin$_{1A}$ (5-HT$_{1A}$) receptor is an important member of the GPCR superfamily and is the most extensively studied of the serotonin receptors for a variety of reasons (*17*). The serotonin$_{1A}$ receptor agonists and antagonists have been shown to possess potential therapeutic effects in anxiety or stress-related disorders (*17*). As a result, the serotonin$_{1A}$ receptor serves as an important target in the development of therapeutic agents for neuropsychiatric disorders such as anxiety and depression. Interestingly, mutant (knockout) mice lacking the serotonin$_{1A}$ receptor exhibit enhanced anxiety-related behavior and represent an important animal model for genetic vulnerability to complex traits such as anxiety disorders and aggression in higher animals (*18*). With the pharmacological relevance of the serotonin$_{1A}$ receptor in mind, the interaction of this transmembrane protein with the lipid environment assumes greater significance in its function in healthy and diseased states.

[†]Supported by research grants from the Council of Scientific and Industrial Research (Government of India) to A.C. A.C. gratefully acknowledges support from a J. C. Bose Fellowship (Department of Science and Technology, Government of India). T.J.P. and S.G. thank the Council of Scientific and Industrial Research for the award of Senior Research Fellowships. Y.D.P. was the recipient of a postdoctoral fellowship from a CSIR Network project on Nanomaterials and Nanodevices (NWP0035). A.C. is an Adjunct Professor at the Special Centre for Molecular Medicine of Jawaharlal Nehru University (New Delhi, India) and Honorary Professor of the Jawaharlal Nehru Centre for Advanced Scientific Research (Bangalore, India).

*To whom correspondence should be addressed: Telephone: +91-40-2719-2578. Fax: +91-40-2716-0311. E-mail: amit@ccmb.res.in.

[1]Abbreviations: 5-HT$_{1A}$ receptor, 5-hydroxytryptamine-1A receptor; 5-HT$_{1A}$R-EYFP, 5-hydroxytryptamine-1A receptor tagged to EYFP; 8-OH-DPAT, 8-hydroxy-2-(di-*N*-propylamino)tetralin; BCA, bicinchoninic acid; DMPC, dimyristoyl-*sn*-glycero-3-phosphocholine; DPH, 1,6-diphenyl-1,3,5-hexatriene; EYFP, enhanced yellow fluorescent protein; FRAP, fluorescence recovery after photobleaching; GPCR, G-protein-coupled receptor; GTP-γ-S, guanosine 5′-*O*-(3-thiotriphosphate); HMG-CoA reductase, 3-hydroxy-3-methylglutaryl coenzyme A reductase; MβCD, methyl-β-cyclodextrin; *p*-MPPF, 4-(2′-methoxy)-phenyl-1-[2′-(*N*-2′′-pyridinyl)-*p*-fluorobenzamido]ethylpiperazine; *p*-MPPI, 4-(2′-methoxy)phenyl-1-[2′-(*N*-2′′-pyridinyl)-*p*-iodobenzamido]ethylpiperazine; PMSF, phenylmethanesulfonyl fluoride.

 Published on Web 06/03/2010

We previously demonstrated the requirement of membrane cholesterol in the function of the serotonin$_{1A}$ receptor (*10*, *19*). This was achieved by physical depletion of cholesterol from membranes using MβCD followed by monitoring receptor function (*19*, *20*). However, membrane cholesterol depletion using MβCD suffers from a number of limitations (*21*). A major limitation is that such cholesterol depletion using MβCD is an acute process due to the relatively short time of treatment. To overcome such limitations, we chose to reduce cellular membrane cholesterol using statins. Such cholesterol depletion takes place over a longer period of time and represents a chronic treatment, thereby mimicking physiological situations. In this work, we have explored the effect of chronic cholesterol depletion using mevastatin on the function of the human serotonin$_{1A}$ receptor, stably expressed in Chinese hamster ovary (termed as CHO-5-HT$_{1A}$R) cells (*22*). Our results show a significant reduction in the level of specific agonist and antagonist binding to the serotonin$_{1A}$ receptor upon chronic cholesterol depletion. Interestingly, we show here that the effect of chronic cholesterol depletion on the ligand binding of serotonin$_{1A}$ receptors is reversible. In addition, fluorescence recovery after photobleaching (FRAP) measurements reveal novel changes in receptor dynamics upon chronic cholesterol depletion. These novel results could have significant implications for our understanding of the influence of cholesterol lowering agents such as statin on the organization and function of the serotonin$_{1A}$ receptor, an important neurotransmitter receptor.

EXPERIMENTAL PROCEDURES

Materials. Cholesterol, $CaCl_2$, DMPC, DPH, EDTA, gentamycin sulfate, MβCD, (±)-mevalonolactone, $MgCl_2$, $MnCl_2$, oleic acid albumin, penicillin, polyethylenimine, *p*-MPPI, PMSF, serotonin, sodium bicarbonate, streptomycin, and Tris were obtained from Sigma Chemical Co. (St. Louis, MO). D-MEM/F-12 [Dulbecco's modified Eagle's medium/nutrient mixture F-12 (Ham) (1:1)], fetal calf serum, and Geneticin (G 418) were from Invitrogen Life Technologies (Carlsbad, CA). GTP-γ-S and Nutridoma-SP were from Roche Applied Science (Mannheim, Germany). BCA reagent for protein estimation was from Pierce (Rockford, IL). Mevastatin was obtained from Calbiochem (San Diego, CA). [^{3}H]-8-OH-DPAT (specific activity of 135.0 Ci/mmol) and [^{3}H]-*p*-MPPF (specific activity of 70.5 Ci/mmol) were purchased from DuPont New England Nuclear (Boston, MA). GF/B glass microfiber filters were from Whatman International (Kent, U.K.). All other chemicals and solvents used were of the highest available purity. Water was purified through a Millipore (Bedford, MA) Milli-Q system and used throughout.

Cell Culture and Mevastatin Treatment. CHO cells stably expressing the human serotonin$_{1A}$ receptor (termed CHO-5-HT$_{1A}$R) and CHO cells stably expressing the human serotonin$_{1A}$ receptor tagged to enhanced yellow fluorescent protein (termed CHO-5-HT$_{1A}$R-EYFP) were maintained in D-MEM/F-12 (1:1) supplemented with 2.4 g/L sodium bicarbonate, 10% fetal calf serum, 60 μg/mL penicillin, 50 μg/mL streptomycin, 50 μg/mL gentamycin sulfate, and 200 μg/mL (300 μg/mL in the case of CHO-5-HT$_{1A}$R-EYFP cells) Geneticin (D-MEM/F-12 complete medium) in a humidified atmosphere with 5% CO_2 at 37 °C. Nutridoma-BO (lipid deficient medium) was prepared using 1% Nutridoma-SP, 0.33 mg/mL oleic acid albumin, 0.1% fetal calf serum, 12 μg/mL penicillin, 10 μg/mL streptomycin, and 10 μg/mL gentamycin sulfate. The stock solution of mevastatin was prepared as described previously (*23*). The final concentrations of mevastatin and mevalonolactone were 50 and 200 μM, respectively. In the case of mevastatin treatment, cells were grown for 56 h in D-MEM/F-12 medium and then shifted to Nutridoma-BO medium containing mevastatin and mevalonolactone for 16 h, in a humidified atmosphere with 5% CO_2 at 37 °C. Control cells were grown for 56 h in D-MEM/F-12 complete medium and then changed to Nutridoma-BO (lipid deficient) medium for 16 h.

Cell Membrane Preparation. Cell membranes were prepared as described previously (*22*). The total protein concentration in the isolated membranes was determined using the BCA assay (*24*).

Estimation of Membrane Cholesterol and Phospholipid Contents. The cholesterol content in cell membranes was estimated using the Amplex Red cholesterol assay kit (*25*). The phospholipid content in these membranes was determined after total digestion with perchloric acid as described previously (*26*) using Na_2HPO_4 as a standard.

Radioligand Binding Assays. Receptor binding assays were conducted as described previously (*22*) with ~40 μg of total protein. Final concentrations of the radiolabeled agonist [^{3}H]-8-OH-DPAT and antagonist [^{3}H]-*p*-MPPF in each assay tube were 0.29 and 0.5 nM, respectively.

Saturation Radioligand Binding Assays. Saturation binding assays were conducted with increasing concentrations (0.1−7.5 nM) of the radiolabeled agonist [^{3}H]-8-OH-DPAT as described previously (*22*). The dissociation constant (K_d) and the number of maximum binding sites (B_{max}) were calculated by nonlinear regression analysis of binding data using Graphpad (San Diego, CA) Prism version 4.00. Data obtained after regression analysis were used to plot graphs with GRAFIT version 3.09b (Erithacus Software, Surrey, U.K.).

GTP-γ-S Sensitivity Assay. To estimate the efficiency of G-protein coupling, we conducted GTP-γ-S sensitivity assays as described previously (*22*). The concentrations of GTP-γ-S leading to 50% inhibition of specific agonist binding (IC_{50}) were calculated by nonlinear regression fitting of the data to a four-parameter logistic function (*27*):

$$B = a/[1 + (x/I)^s] + b \quad (1)$$

where B is the specific binding of the agonist normalized to agonist binding at the lowest concentration of GTP-γ-S, x denotes the concentration of GTP-γ-S, a is the range ($y_{max} - y_{min}$) of the fitted curve on the ordinate (y-axis), I is the IC_{50} concentration, b is the background of the fitted curve (y_{min}), and s is the slope factor.

Fluorescence Anisotropy Measurements. Fluorescence anisotropy experiments were conducted using the membrane probe DPH with membranes prepared from cells (treated with mevastatin and cholesterol-replenished) containing 50 nmol of total phospholipids suspended in 1.5 mL of 50 mM Tris buffer (pH 7.4), as described previously (*28*). Steady state fluorescence was measured in a Hitachi F-4010 spectrofluorometer using 1 cm path length quartz cuvettes at room temperature (~23 °C). Excitation and emission wavelengths were set at 358 and 430 nm, respectively. Excitation and emission slits with nominal band passes of 1.5 and 20 nm, respectively, were used. The optical density of the samples measured at 358 nm was always less than 0.1. Fluorescence anisotropy measurements were performed using a Hitachi polarization accessory. Anisotropy (r) values were calculated

from the following equation (*29*):

$$r = \frac{I_{VV} - GI_{VH}}{I_{VV} + 2GI_{VH}} \quad (2)$$

where I_{VV} and I_{VH} are the measured fluorescence intensities (after appropriate background subtraction) with the excitation polarizer vertically oriented and the emission polarizer vertically and horizontally oriented, respectively. G is the grating correction factor that corrects for wavelength-dependent distortion of the polarizers and is the ratio of the efficiencies of the detection system for vertically and horizontally polarized light, equal to I_{HV}/I_{HH}. All experiments were conducted with multiple sets of samples, and average values of fluorescence anisotropy are shown in Figure 5.

Cholesterol Replenishment with the Cholesterol−MβCD Complex. Following treatment with mevastatin, cells were incubated with the cholesterol−MβCD complex for 5 min in a humidified atmosphere with 5% CO_2 at 37 °C. The complex was prepared by dissolving the required amounts of cholesterol and MβCD in a ratio of 1:10 (molar ratio) in water by constant vortexing at room temperature (~23 °C). Stock solutions (typically 2 mM cholesterol and 20 mM MβCD) of this complex were freshly prepared and were added to 2× DMEM/F-12 (1:1) medium without fetal calf serum, yielding final concentrations of 1 mM cholesterol and 10 mM MβCD.

Western Blot Analysis. Cell membranes were prepared from CHO-5-HT_{1A}R-EYFP (control), mevastatin-treated, and cholesterol-replenished cells as previously described (*22*), with an addition of a 1:20 dilution of freshly prepared protease inhibitor cocktail (Roche Applied Science, Mannheim, Germany). Total protein (60 μg) from each sample was mixed with electrophoresis sample buffer and incubated for 30 min at 37 °C. Sample mixtures were loaded and separated via 10% SDS−PAGE. After electrophoresis, proteins were electrophoretically transferred to a nitrocellulose membrane (Hybond ECL, Amersham Pharmacia Biotech, Little Chalfont, U.K.) using a semidry transfer apparatus (Amersham Pharmacia Biotech). The nonspecific binding sites were blocked with 10% fat-free dry milk in PBS with Tween 20 (pH 7.4) for 1 h at room temperature (~23 °C). To monitor the expression of 5-HT_{1A}R-EYFP, blots were probed with antibodies raised against GFP (Abcam, Cambridge, U.K.; 1:1500 dilution in PBS with Tween 20) and incubated for 90 min at room temperature (~23 °C). To monitor the levels of β-actin, which acts as a loading control, membranes were probed with antibodies raised against β-actin (Chemicon International, Temecula, CA; diluted 1:3000 in PBS with Tween 20) and incubated for 90 min at room temperature (~23 °C). Membranes were washed with PBS and Tween 20 (washing buffer) for 15 min, and the washing buffer was changed every 5 min. Membranes were then incubated with a 1:4000 dilution of respective secondary antibodies (horseradish peroxidase-conjugated anti-rabbit antibody for 5-HT_{1A}R-EYFP and horseradish peroxidase-conjugated anti-mouse antibody for β-actin) in PBS and Tween 20 for 45 min at room temperature (~23 °C). Membranes were then washed and developed using the enhanced chemiluminescence detection reagents (Amersham Biosciences, Buckinghamshire, U.K.). 5-HT_{1A}R-EYFP and β-actin were detected using the chemiluminescence detection system (Chemi-Smart 5000, Vilber Lourmat). 5-HT_{1A}R-EYFP and β-actin levels were quantitated using Bio-Profile (Bio-1D+, version 11.9).

Fluorescence Recovery after Photobleaching (FRAP) Measurements and Analysis. FRAP experiments were conducted with cells that were grown in medium for 72 h [56 h in D-MEM/F-12 complete medium followed by change of medium to Nutridoma-BO for 16 h (lipid deficient medium)] on Lab-Tek chambered coverglass (Nunc). In the case of mevastatin treatment, cells were grown in Nutridoma-BO medium containing mevastatin and mevalonolactone for 16 h. After this treatment, cells were washed with buffer A [PBS containing 1 mM $CaCl_2$ and 0.5 mM $MgCl_2$ (pH 7.4)]. Fluorescence images were acquired at room temperature (~23 °C), on an inverted Zeiss (Jena, Germany) LSM 510 Meta confocal microscope, with a 63×, 1.2 NA water immersion objective using the 514 nm line of an argon laser, and a 535−590 nm filter for the collection of EYFP fluorescence. Images were recorded with a pinhole of 225 μm, giving an optimal z-slice thickness of 1.7 μm. The distinct membrane fluorescence of the cell periphery was targeted for bleaching and monitoring of fluorescence recovery (*20*, *30*). Analysis with a control region of interest (ROI) drawn a certain distance from the bleach ROI indicated no significant bleach while fluorescence recovery was monitored (see Figure 8). Data representing the mean fluorescence intensity of the bleached ROI (~1.4 μm radius) were background subtracted using a ROI placed outside the cell. Fluorescence recovery plots with fluorescence intensities normalized to prebleach intensities were analyzed according to the uniform disk illumination condition (*31*):

$$F(t) = [F(\infty) - F(0)]\{\exp(-2\tau_d/t)[I_0(2\tau_d/t) + I_1(2\tau_d/t)]\} + F(0) \quad (3)$$

where $F(t)$ is the mean background-corrected and normalized fluorescence intensity at time t in the bleached ROI, $F(\infty)$ is the recovered fluorescence at time ∞, $F(0)$ is the bleached fluorescence intensity set at time zero, and τ_d is the characteristic diffusion time. I_0 and I_1 are modified Bessel functions. The diffusion coefficient (D) is determined from the equation

$$D = \omega^2/4\tau_d \quad (4)$$

where ω is the actual radius of the bleached ROI. Mobile fraction (R) estimates of the fluorescence recovery were obtained from the equation

$$R = [F(\infty) - F(0)]/[1 - F(0)] \quad (5)$$

where the mean background-corrected and normalized prebleach fluorescence intensity is equal to unity. Normalized intensities of each data set were fitted individually to eq 3, and parameters derived were used in eqs 4 and 5. Statistical analysis was performed on the entire set of derived parameters for all given conditions.

Nonlinear Curve Fitting and Statistical Analysis. Significance levels were estimated using a Student's two-tailed unpaired t test using Graphpad Prism version 4.00. Nonlinear curve fitting of the fluorescence recovery data to eq 3 was conducted using Graphpad Prism version 4.00. Origin version 5.0 (OriginLab Corp., Northampton, MA) was used for the frequency distribution plot and analysis.

RESULTS

Chronic Cholesterol Depletion upon Statin Treatment. CHO-5-HT_{1A}R cells stably expressing the human serotonin$_{1A}$ receptor were treated with mevastatin to achieve chronic depletion of cholesterol. Statins are powerful inhibitors of HMG-CoA reductase, the key enzyme in cholesterol biosynthesis that catalyzes

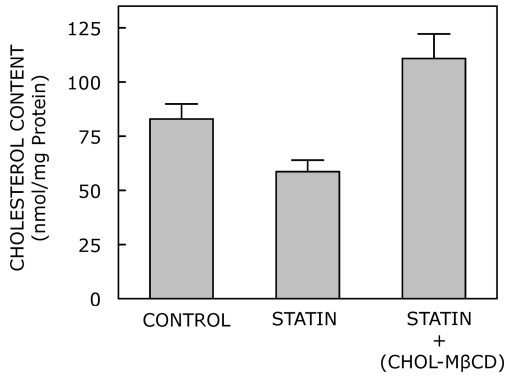

FIGURE 1: Cholesterol content of membranes isolated from CHO-5-HT_{1A}R cells. Cholesterol content was estimated in membranes isolated from CHO-5-HT_{1A}R cells treated with mevastatin and replenished with cholesterol. Values are expressed as nanomoles of cholesterol per milligram of protein. Data represent means ± the standard error from four independent measurements. See Experimental Procedures for other details.

the rate-limiting step in the biosynthetic pathway (*13*). Figure 1 shows that ~30% of the cholesterol is depleted in CHO-5-HT_{1A}R cells treated with mevastatin. Upon treatment with the cholesterol−MβCD complex, the cholesterol content is increased to ~134% of the control. The cholesterol contents shown in Figure 1 are in good agreement with literature values (*32*, *33*). Importantly, the membrane phospholipid content of cells either treated with mevastatin or replenished with cholesterol remains unaltered (data not shown), indicating that these treatments are specific to cholesterol.

The Level of Ligand Binding of the Human Serotonin$_{1A}$ Receptor Is Reduced upon Chronic Cholesterol Depletion. We explored the ligand binding function of the human serotonin$_{1A}$ receptor upon statin treatment. For this, we measured the binding of the selective serotonin$_{1A}$ receptor agonist [^{3}H]-8-OH-DPAT and antagonist [^{3}H]-*p*-MPPF to membranes isolated from CHO-5-HT_{1A}R cells treated with mevastatin and replenished with cholesterol. Figure 2A shows that chronic cholesterol depletion with statin reduced the level of specific agonist [^{3}H]-8-OH-DPAT binding to serotonin$_{1A}$ receptors to ~54% of the original value [due to ~30% cholesterol depletion (see above)]. The corresponding value for specific antagonist [^{3}H]-*p*-MPPF binding following statin treatment was ~59% (Figure 2B). To the best of our knowledge, these results represent the first report of inhibition of specific ligand binding to serotonin$_{1A}$ receptors due to chronic cholesterol depletion using statin. Importantly, the reduction in the level of ligand binding is not due to a decrease in the expression level of the human serotonin$_{1A}$ receptor (see later, Figure 7).

To check the reversibility of the effect of chronic cholesterol depletion on ligand binding of the serotonin$_{1A}$ receptor, cholesterol replenishment of mevastatin-treated cells was conducted via treatment with the cholesterol−MβCD complex as described in Experimental Procedures. As shown in Figure 1, this procedure was able to load back cholesterol to the cells as shown by the cholesterol content of the replenished cell membranes. The corresponding recovery in ligand binding is shown in Figure 2. This shows that the loss of ligand binding was indeed due to membrane cholesterol depletion.

The saturation binding analysis of the specific agonist [^{3}H]-8-OH-DPAT binding to serotonin$_{1A}$ receptors is shown in Figure 3 and Table 1. The results of saturation binding analysis, conducted

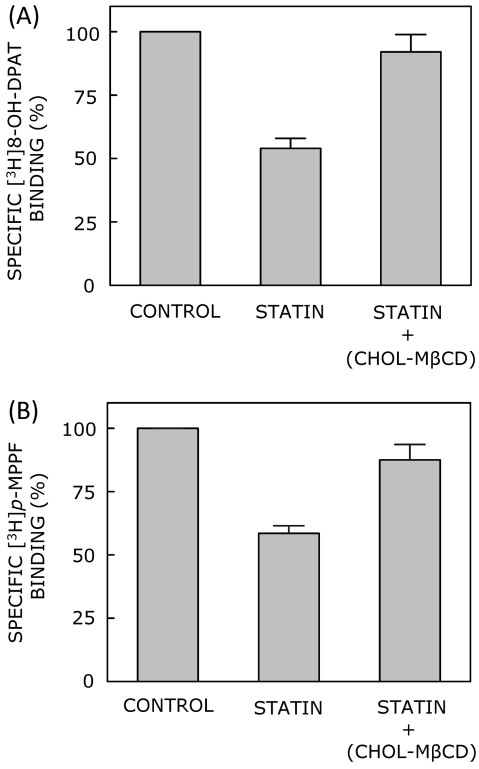

FIGURE 2: Inhibition of ligand binding of the human serotonin$_{1A}$ receptor upon chronic cholesterol depletion. Specific binding of the agonist [^{3}H]-8-OH-DPAT (A) and the antagonist [^{3}H]-*p*-MPPF (B), to the human serotonin$_{1A}$ receptor in membranes isolated from CHO-5-HT_{1A}R cells treated with mevastatin and replenished with cholesterol, is shown. Values are expressed as percentages of specific ligand binding obtained in control cell membranes. Data shown are means ± the standard error from at least four independent measurements. See Experimental Procedures for other details.

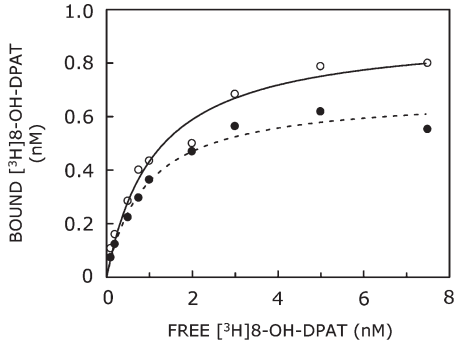

FIGURE 3: Saturation binding analysis of specific [^{3}H]-8-OH-DPAT binding to serotonin$_{1A}$ receptors in membranes isolated from control and statin-treated CHO-5-HT_{1A}R cells. Representative plots are shown for specific [^{3}H]-8-OH-DPAT binding with increasing concentrations of [^{3}H]-8-OH-DPAT under control (○) and statin-treated (●) conditions. See Experimental Procedures and Table 1 for other details.

with membranes prepared from control and statin-treated cells, revealed that the reduction in the level of ligand binding can primarily be attributed to a reduction in the number of total binding sites with a marginal reduction in the affinity of ligand binding. There is a significant reduction (~35%, $p < 0.05$) in the maximum number of binding sites (B_{max}) when the CHO-5-HT_{1A}R cells were treated with statin. The binding affinity of [^{3}H]-8-OH-DPAT in statin-treated cell membranes in the presence of 1 nM GTP-γ-S is given in the Supporting Information (see Table S1).

Table 1: Effect of Statin Treatment on Specific [^{3}H]-8-OH-DPAT Binding Parameters[a]

experimental condition	K_d (nM)	B_{max} (pmol/mg of protein)
control	1.03 ± 0.09	0.89 ± 0.07
mevastatin	0.87 ± 0.02	0.58 ± 0.08

[a]Binding parameters were calculated by analyzing saturation binding isotherms with a range of [^{3}H]-8-OH-DPAT concentrations using Graphpad Prism. Data represent means ± the standard error of duplicate points from at least three independent measurements. See Experimental Procedures for other details.

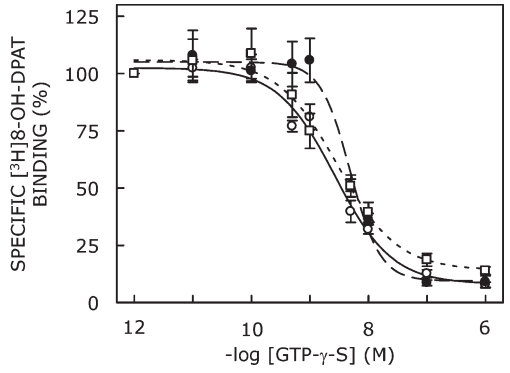

FIGURE 4: Reduced level of G-protein coupling of the human serotonin$_{1A}$ receptor upon treatment with mevastatin. The G-protein coupling efficiency of the serotonin$_{1A}$ receptor was monitored by the sensitivity of [^{3}H]-8-OH-DPAT binding in the presence of GTP-γ-S. The figure shows the effect of increasing concentrations of GTP-γ-S on the specific binding of the agonist [^{3}H]-8-OH-DPAT to serotonin$_{1A}$ receptors in membranes isolated from control (○), mevastatin-treated (●), and cholesterol-replenished (□) cells. Values are expressed as percentages of specific binding obtained at the lowest concentration of GTP-γ-S. The curves are nonlinear regression fits to the experimental data using eq 1. Data points represent means ± the standard error of duplicate points from at least four independent experiments. See Experimental Procedures for other details.

Table 2: Effect of Chronic Cholesterol Depletion on the Efficiency of G-Protein Coupling[a]

experimental condition	IC_{50} (nM)
control	2.77 ± 0.43
mevastatin	4.85 ± 0.12
mevastatin with the cholesterol−MβCD complex	2.97 ± 0.54

[a]The sensitivity of specific [^{3}H]-8-OH-DPAT binding in the presence of GTP-γ-S in the assay was measured by calculating the IC_{50} for inhibition of [^{3}H]-8-OH-DPAT binding in the presence of a range of concentrations of GTP-γ-S. Inhibition curves were analyzed using the four-parameter logistic function. Data represent means ± the standard error of four independent experiments. See Experimental Procedures for other details.

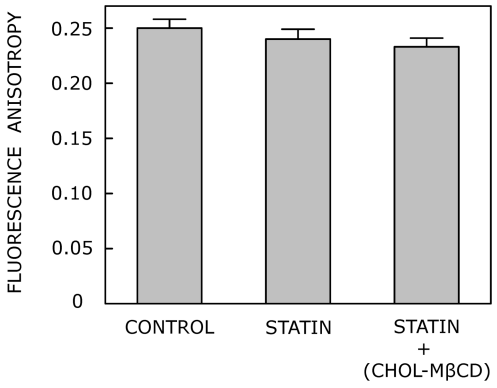

FIGURE 5: Overall membrane order is unaltered upon chronic cholesterol depletion. Overall (average) membrane order was estimated in membranes isolated from cells treated with mevastatin and replenished with cholesterol, using the fluorescence anisotropy of the membrane probe DPH. Fluorescence anisotropy measurements were taken with membranes containing 50 nmol of phospholipid at a probe:phospholipid molar ratio of 1:100 at room temperature (~23 °C). Data represent means ± the standard error from at least four independent experiments. See Experimental Procedures for other details.

G-Protein Coupling Efficiency of the Human Serotonin$_{1A}$ Receptor Is Reduced upon Statin Treatment. Most of the seven transmembrane domain receptors are coupled to G-proteins, and therefore, guanine nucleotides are known to modulate ligand binding. The serotonin$_{1A}$ receptor agonists such as 8-OH-DPAT are known to specifically activate the G_i/G_o class of G-proteins in CHO cells (*34*). Agonist binding to such receptors therefore displays sensitivity to agents such as GTP-γ-S, a nonhydrolyzable analogue of GTP, that uncouple the normal cycle of guanine nucleotide exchange at the Gα subunit caused by receptor activation. We have previously shown that in the presence of GTP-γ-S, serotonin$_{1A}$ receptors undergo an affinity transition, from a high-affinity G-protein-coupled state to a low-affinity G-protein-uncoupled state (*35*). In agreement with these results, Figure 4 shows a characteristic reduction in the level of binding of the agonist [^{3}H]-8-OH-DPAT in the presence of increasing concentrations of GTP-γ-S with an estimated half-maximal inhibition concentration (IC_{50}) of 2.77 nM for control cells (see Table 2). The inhibition curve in the case of cells treated with mevastatin displays a significant ($p < 0.05$) shift toward higher concentrations of GTP-γ-S with an increased IC_{50} value of 4.85 nM. This implies that the agonist binding to the serotonin$_{1A}$ receptor in mevastatin-treated cells is less sensitive to GTP-γ-S, indicating that the G-protein coupling efficiency is reduced under these conditions. This suggests a possible perturbation of receptor−G-protein interaction under chronic cholesterol-depleted conditions. Interestingly, Table 2 shows that the IC_{50} value is restored (2.97 nM) upon subsequent cholesterol replenishment.

Reduction in the Function of the Human Serotonin$_{1A}$ Receptor due to Statin Treatment Is Independent of the Overall Membrane Order. To explore any possible change in overall membrane order upon mevastatin treatment, we measured the fluorescence anisotropy of the membrane probe DPH. Fluorescence anisotropy measured using probes such as DPH is correlated to the rotational diffusion of membrane-embedded probes (*29*), which is sensitive to the packing of lipid fatty acyl chains. This is due to the fact that fluorescence anisotropy depends on the degree to which the probe is able to reorient after excitation, and probe reorientation is a function of local lipid packing. DPH, which is a rodlike hydrophobic molecule, partitions into the interior (fatty acyl chain region) of the bilayer. Figure 5 shows the effect of chronic cholesterol depletion and cholesterol replenishment on fluorescence anisotropy of the membrane probe DPH incorporated into CHO-5-HT$_{1A}$R cell membranes. Fluorescence anisotropy of DPH appears to be predominantly invariant in membranes isolated from control, mevastatin-treated, and cholesterol-replenished cells. These results therefore suggest that the overall membrane order, as reported by DPH anisotropy, is not significantly altered under mevastatin-treated and cholesterol-replenished conditions. It should be noted here that

Table 3: Diffusion Coefficients and Mobile Fractions of 5-HT_{1A}R-EYFP upon Mevastatin Treatment[a]

	control (N = 38)	mevastatin (N = 42)	p value (for mean)	p value (for F test)
diffusion coefficient ($\mu m^2/s$)	0.27 ± 0.03	0.17 ± 0.02	< 0.05	< 0.05
mobile fraction (%)	63.9 ± 1.54	68.3 ± 1.54	< 0.05	–

[a] N represents the number of independent measurements, and data shown are means ± the standard error. A two-tailed, unpaired Student's t test was performed on diffusion coefficient and mobile fraction estimates, and the corresponding p values are given. In both cases, differences in values were found to be significant. To estimate differences in population variance, an F test was performed. The population variance with respect to diffusion coefficient was found to be significantly different between control and mevastatin-treated cells ($p < 0.05$; see the text for details). See Experimental Procedures for other details.

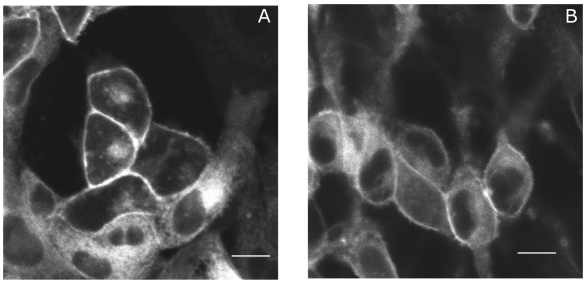

FIGURE 6: Cellular morphology and overall distribution of 5-HT_{1A}R-EYFP that remain unaltered in control and mevastatin-treated cells. Panels A and B show typical fluorescence distributions of 5-HT_{1A}R-EYFP in CHO cells in control and mevastatin-treated cells, respectively. Fluorescence images of cells grown on a Lab-Tek chambered coverglass system were acquired at room temperature (~23 °C) in the presence of buffer A. The images represent midplane confocal sections of the cells under conditions described in Experimental Procedures. The scale bar represents 10 μm. See Experimental Procedures for other details.

membrane dynamics reported by anisotropy reflects relatively fast time scale (nanoseconds) and short-range (local) events. The corresponding changes in long-range lateral dynamics over slower time scales are discussed later (Table 3 and Figure 9).

The Cellular Morphology and Overall Fluorescence Distribution of EYFP-Tagged Serotonin$_{1A}$ Receptors Remain Unaltered upon Mevastatin Treatment. We have previously shown that fusion of EYFP to the serotonin$_{1A}$ receptor does not affect the ligand binding property, G-protein coupling, or signaling function of the receptor (*36*). CHO cells stably expressing 5-HT_{1A}R-EYFP therefore represent a reliable system for exploring the membrane organization and dynamics of the serotonin$_{1A}$ receptor. In addition, the EYFP variant is particularly suitable since it is relatively photostable and has a high quantum yield (*36*, *37*). The fluorescence distribution of 5-HT_{1A}R-EYFP in CHO-5-HT_{1A}R-EYFP cells was recorded in control cells and cells treated with mevastatin (shown in Figure 6). Analyses of several independent images acquired with control and mevastatin-treated cells do not indicate a significant redistribution of fluorescence of 5-HT_{1A}R-EYFP.

The Membrane Expression Level of the Serotonin$_{1A}$ Receptor Is Not Reduced under Chronic Cholesterol-Depleted Condition. The impaired ligand binding and G-protein coupling of the serotonin$_{1A}$ receptor observed upon mevastatin treatment could be due to reduced expression levels of serotonin$_{1A}$ receptors. To examine this possibility, we performed Western blot analysis of 5-HT_{1A}R-EYFP in cell membranes prepared from control, mevastatin-treated, and cholesterol-replenished CHO-5-HT_{1A}R-EYFP cells (see Figure 7). For these experiments, we chose to use the receptor tagged with EYFP (5-HT_{1A}R-EYFP) since no monoclonal antibodies for the serotonin$_{1A}$ receptor are available yet, and the polyclonal antibodies have been reported to

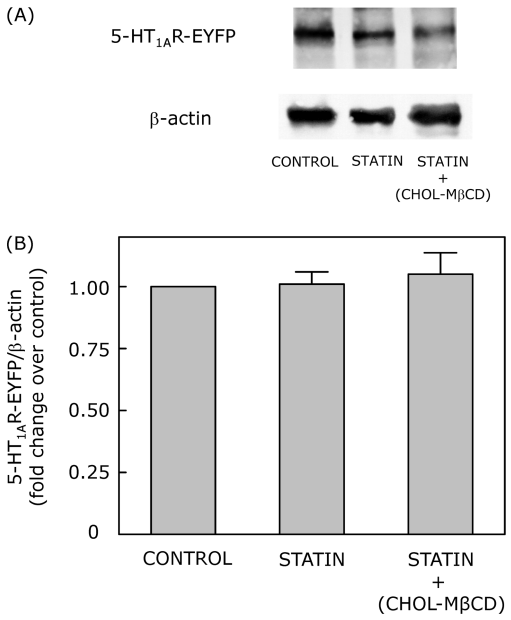

FIGURE 7: Expression level of the human serotonin$_{1A}$ receptor which is not altered in membranes upon chronic cholesterol depletion. Western blot analysis of 5-HT_{1A}R-EYFP in membranes prepared from control, mevastatin-treated, and cholesterol-replenished CHO-5-HT_{1A}R-EYFP cells. Panel A shows the human serotonin$_{1A}$ receptor tagged with EYFP with corresponding β-actin probed with antibodies directed against GFP and β-actin. Panel B shows the quantitation of 5-HT_{1A}R-EYFP and β-actin levels using densitometry. 5-HT_{1A}R-EYFP levels were normalized to β-actin of the corresponding sample. Data are shown as the fold change in 5-HT_{1A}R-EYFP over control and represent means ± the standard error of at least four independent experiments. See Experimental Procedures for other details.

give variable results on Western blots (*38*). As mentioned earlier, we have shown that fusion of EYFP to the serotonin$_{1A}$ receptor does not affect ligand binding, G-protein coupling, or signaling of the receptor (*36*). Figure 7 shows that the levels of the serotonin$_{1A}$ receptor in membranes are not reduced upon mevastatin treatment and cholesterol replenishment.

Lateral Dynamics of the Serotonin$_{1A}$ Receptor upon Chronic Cholesterol Depletion. Fluorescence recovery after photobleaching involves generation of a concentration gradient of fluorescent molecules by irreversible photobleaching of a fraction of fluorophores in the sample region. The dissipation of this gradient with time because of diffusion of fluorophores into the bleached region from the unbleached regions in the membrane is an indicator of the mobility of the fluorophores in the membrane. Representative images showing the recovery of fluorescence intensity after photobleaching are shown in Figure 8A–D. A typical fluorescence recovery plot with regression fits to the data is shown in Figure 8E. A large data set was collected keeping in mind the inherent statistical variation in biological membranes. Figure 9

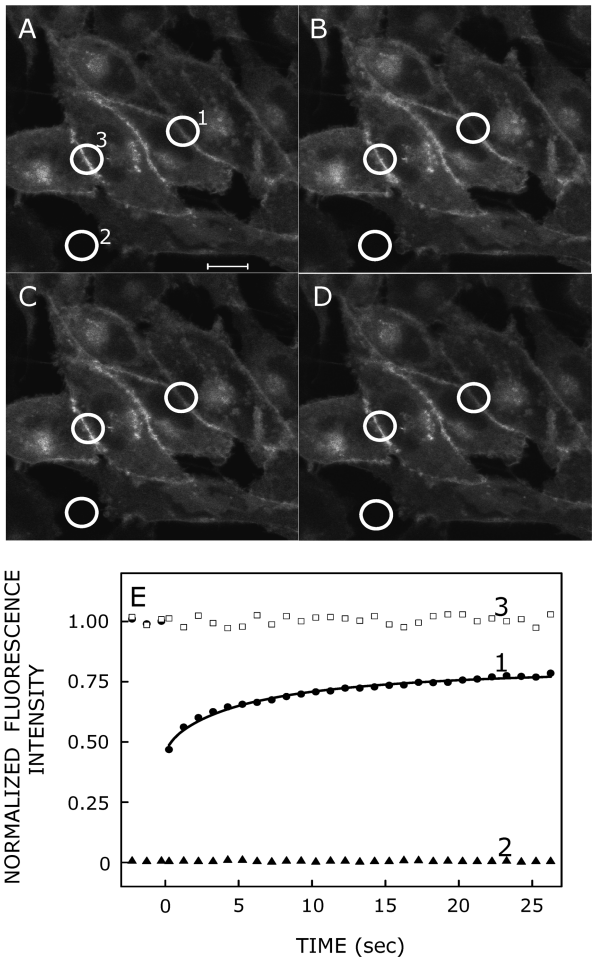

FIGURE 8: Recovery of fluorescence intensity after photobleaching of 5-HT_{1A}R-EYFP. The cellular periphery with clear plasma membrane localization of 5-HT_{1A}R-EYFP was targeted for FRAP experiments. Typical images corresponding to prebleach (A), bleach (B), immediate postbleach (C). and complete recovery (D) are shown. Panel E shows a representative set of normalized fluorescence intensity values of 5-HT_{1A}R-EYFP (●) corresponding to ROI 1 and normalized background intensity (▲) corresponding to ROI 2. The normalized fluorescence intensity in the control ROI 3 (□) was monitored for the same time period and indicates no significant photobleaching due to repeated scanning of the region. The dimensions of ROIs shown are merely representative. The solid line tracing the recovery is the fit of the data to eq 3. The scale bar represents 10 μm. See Experimental Procedures for details.

shows the frequency distribution histograms of diffusion coefficients (panels A and B) and mobile fractions (panels C and D) of 5-HT_{1A}R-EYFP in control and mevastatin-treated cells, and a summary of FRAP data is given in Table 3. The diffusion coefficient of 5-HT_{1A}R-EYFP shows a significant (~37%, $p < 0.05$) reduction upon mevastatin treatment (Table 3 and Figure 9A,B). It should be noted that the distribution of diffusion coefficients in the case of control cells (Figure 9A) exhibits a higher variance (see Table 3), indicating the dynamic heterogeneity of the FRAP time scale (approximately seconds) in the cell membrane. Interestingly, the distribution of diffusion coefficients becomes predominantly homogeneous upon chronic cholesterol depletion. This is consistent with earlier observations that cholesterol depletion leads to a reduction in cholesterol-induced heterogeneity and results in a relatively homogeneous membrane (*39*). The mobile fraction of 5-HT_{1A}R-EYFP, on the other hand, shows a small yet significant (~7%, $p < 0.05$) increase in its mean value upon mevastatin treatment (Table 3 and Figures 9C,D). Interestingly, a similar reduction in the diffusion coefficient and an increase in the mobile fraction have previously been reported upon cholesterol depletion (*40*, *41*).

DISCUSSION

Lipid−protein interactions play an important role in maintaining the structure and function of integral membrane proteins and receptors (*42*−*44*). Specific lipid requirements for the function of membrane proteins have made the choice of a suitable host system for heterologous expression of membrane proteins more challenging (*45*). A possible role of lipids in a variety of neurological disorders is well-documented (*46*). For example, several epidemiological studies indicate a possible role of lipids in a variety of neurological disorders that have been shown to involve deregulated lipid metabolism (*47*). A large portion of any given transmembrane receptor remains in contact with the membrane lipid environment. This raises the obvious possibility that the membrane could be an important modulator of receptor structure and function. Monitoring such lipid−receptor interactions is of particular importance since cells have the ability to vary their membrane lipid composition in response to a variety of stress and stimuli, thereby changing the environment and activity of receptors. Considering the diverse array of lipids in natural membranes, it is believed that physiologically relevant processes occurring in membranes involve an intense coordination of multiple lipid−protein interactions. Cholesterol is an important lipid in this context since it is known to regulate the function of membrane receptors (*9*), in particular neuronal receptors (*10*, *11*), thereby affecting neurotransmission and possibly giving rise to mood and anxiety disorders (*48*).

The effect of cholesterol on the structure and function of integral membrane proteins and receptors has been a subject of intense investigation (*9*, *10*, *49*). It has been proposed that cholesterol can modulate the function of GPCRs either (i) through a direct (specific) interaction with GPCRs, which could induce a conformational change in the receptor, (ii) through an indirect way by altering the membrane physical properties in which the receptor is embedded, or (iii) through a combination of both. We have recently proposed that cholesterol may occupy "nonannular" binding sites around the serotonin$_{1A}$ receptor (*50*). Nonannular sites are characterized by lack of accessibility to the annular lipids; i.e., these sites cannot be displaced by competition with annular lipids. The locations of the nonannular sites are believed to be either inter- or intramolecular protein interfaces, characterized as deep clefts (or cavities) on the protein surface. Interestingly, the crystal structure of the β_2-adrenergic receptor has recently been reported to have specific cholesterol binding site(s) (*51*). The observed reduction in the level of ligand binding upon statin treatment could therefore be due to a lack of cholesterol in the putative binding sites of the serotonin$_{1A}$ receptor, a reduction in the level of G-protein coupling (Figure 4), or a combination of both.

The reduction in the diffusion coefficient of the receptor upon statin treatment merits comment. The role of membrane cholesterol in the regulation of molecular mobility on the plasma membrane is an active area of research in membrane biology. Nonetheless, a consensus about the dependence of the mobility of membrane-bound molecules on cholesterol levels of the plasma membrane is still lacking. Although cholesterol depletion has been shown to suppress mobility in cellular membranes in some cases (*40*, *41*, *52*, *53*), it was found to be dependent on the length

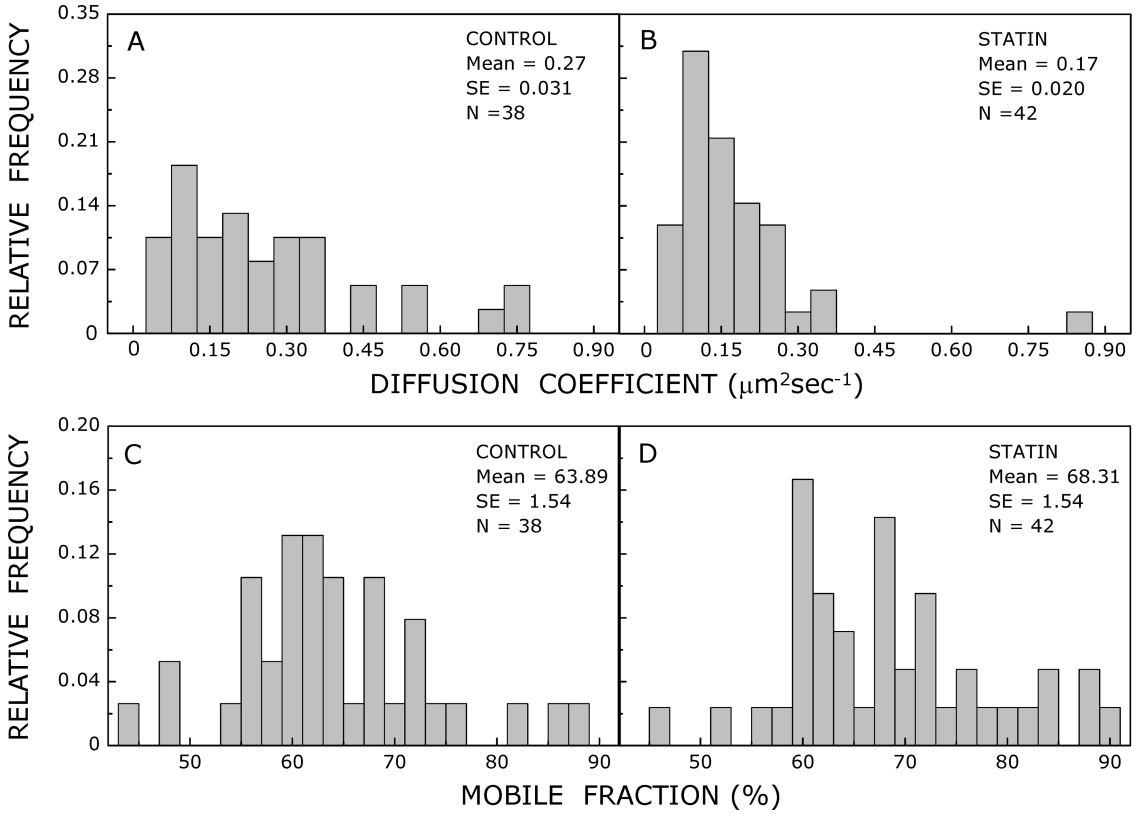

FIGURE 9: Frequency distribution histograms of the diffusion coefficient and mobile fraction of 5-HT_{1A}R-EYFP determined by FRAP. The frequency distribution histograms are obtained by fitting the normalized recovery data of individual experiments to eq 3. Panels A and B show the distribution of the diffusion coefficient, while panels C and D show the distribution of the mobile fraction for control and mevastatin-treated cells, respectively. Means and standard errors are shown in all cases. *N* denotes the number of independent measurements performed in each case. The distributions of diffusion coefficient and mobile fraction were assumed to be unimodal for *F* test analysis. Note that the distribution of diffusion coefficients in the case of mevastatin-treated cells appears to be significantly tighter compared to the corresponding distribution in control cells. See Table 3 and Experimental Procedures for other details.

scales probed (*20*). On the other hand, it has been observed that cholesterol depletion could lead to an increase in molecular mobility (*53*−*55*). In addition, it has been reported that cholesterol depletion could induce alterations in the submembrane actin cytoskeleton via a phosphatidylinositol 4,5-bisphosphate [PI(4,5)P2]-dependent mechanism (*56*). It is possible that the observed increase in the mobile fraction of the receptor is mediated by altered anchorage of this transmembrane protein to the submembrane actin cytoskeleton (ref *57* and unpublished observations of S. Ganguly and A. Chattopadhyay).

The cellular cholesterol content is stringently regulated, and cells that divide retain all the enzymes necessary for biosynthesis of cholesterol. In humans, ~70% of the total cholesterol comes from de novo biosynthesis (*58*). The microsomal enzyme HMG-CoA reductase is the major rate-limiting enzyme in cholesterol biosynthesis. This fact makes this enzyme a popular target for pharmacological regulation of cholesterol synthesis. We have used mevastatin, a fungal metabolite isolated and purified from *Penicillium citrinum* (*59*) that acts as a potent and specific inhibitor of HMG-CoA reductase. In this work, we have explored the effect of chronic cholesterol depletion using mevastatin on the function of the human serotonin$_{1A}$ receptor heterologously expressed in CHO cells. An advantage of using statins to lower the cellular cholesterol level is the fact that cholesterol depletion is chronic which mimics physiological conditions, in contrast to agents such as MβCD that induce acute cholesterol depletion. Our results show a decrease in the cholesterol content of CHO-5-HT_{1A}R cells upon treatment with mevastatin, which leads to a significant reduction in the level of specific ligand binding and G-protein coupling to the serotonin$_{1A}$ receptor, although the membrane receptor level does not exhibit any reduction. Interestingly, replenishment of CHO-5-HT_{1A}R cells with cholesterol resulted in the recovery of specific ligand binding and G-protein coupling. Treatment of CHO cells expressing the serotonin$_{1A}$ receptor tagged with EYFP with mevastatin led to a significant decrease in diffusion coefficient and an increase in the mobile fraction of the receptor, as determined by FRAP measurements. Since statin treatment is associated with neurological disorders (*60*), exploring the function of neuronal receptors and their membrane lipid interactions under these conditions is significant.

Interestingly, a strong asymmetry exists even in the manner in which cholesterol is distributed among various organs in the body of higher eukaryotes. For example, the central nervous system, which accounts for only 2% of the body mass, contains ~25% of free cholesterol present in the whole body (*46*). Although the brain is highly enriched in cholesterol and important neuronal processes such as synaptogenesis require cholesterol (*61*), the organization and dynamics of brain cholesterol are still poorly understood. Brain cholesterol is synthesized in situ and is developmentally regulated. The organization, traffic, and dynamics of brain cholesterol are stringently controlled since the input of cholesterol into the central nervous system is almost exclusively from in situ synthesis as there is no evidence of the transfer of cholesterol from blood plasma to brain (*62*). As a result, a number of neurological diseases share a common etiology of defective cholesterol metabolism in the brain (*47*). The recent increase in

the number of studies in understanding the mechanisms by which cholesterol metabolism in the brain is regulated could be attributed to the fact that defects in cholesterol homeostasis in the brain have been linked to the development of several neurological disorders such as Alzheimer's disease, Niemann-Pick type C disease, and Smith-Lemli-Opitz syndrome (SLOS) (*63*). For example, the marked abnormalities in brain development and function leading to serious neurological and mental dysfunctions in SLOS have their origin in the fact that the major input of brain cholesterol comes from the in situ synthesis and such synthesis is defective in this syndrome (*64*). Interestingly, we have recently shown that the function of the serotonin$_{1A}$ receptor is impaired under conditions mimicking SLOS (*28*). In view of the importance of cholesterol in relation to membrane domains (*3*, *4*), the effect of an alteration in the cholesterol content of neuronal membranes on membrane dynamics and receptor function could represent an important determinant in the analysis of neurogenesis and neuropathology. Although we have used CHO cells in this study, a potential implication of our results is that the interaction between cholesterol and neurotransmitter receptors such as the serotonin$_{1A}$ receptor could be crucial in the brain.

Our results could have significant implications for our understanding of the influence of cholesterol lowering agents such as statin on the function and dynamics of the serotonin$_{1A}$ receptor, in particular, and other G-protein-coupled receptors, in general. These results assume broader significance in the context of previous observations that symptoms of anxiety and major depression are apparent in humans upon long-term statin administration (*48*) and cortical cholesterol content is found to be lower in mood disorders (*65*). This is relevant since some statins have been reported to cross the blood−brain barrier (*66*) and statin use has been associated with a reduced risk of Alzheimer's disease (*67*).

ACKNOWLEDGMENT

We thank members of our laboratory for critically reading the manuscript. We thank Bh Muralikrishna for useful discussions.

SUPPORTING INFORMATION AVAILABLE

Effect of statin treatment on specific [^{3}H]-8-OH-DPAT binding parameters calculated by analyzing saturation binding isotherms with a range of radiolabeled [^{3}H]-8-OH-DPAT concentrations in the presence of 1 nM GTP-γ-S using Graphpad Prism. This material is available free of charge via the Internet at http://pubs.acs.org.

REFERENCES

1. Simons, K., and Ikonen, E. (2000) How cells handle cholesterol. *Science 290*, 1721–1725.
2. Mouritsen, O. G., and Zuckermann, M. J. (2004) What's so special about cholesterol? *Lipids 39*, 1101–1113.
3. Mukherjee, S., and Maxfield, F. R. (2004) Membrane domains. *Annu. Rev. Cell Dev. Biol. 20*, 839–866.
4. Lingwood, D., and Simons, K. (2010) Lipid rafts as a membrane-organizing principle. *Science 327*, 46–50.
5. Simons, K., and van Meer, G. (1988) Lipid sorting in epithelial cells. *Biochemistry 27*, 6197–6202.
6. Simons, K., and Toomre, D. (2000) Lipid rafts and signal transduction. *Nat. Rev. Mol. Cell Biol. 1*, 31–39.
7. Riethmüller, J., Riehle, A., Grassmé, H., and Gulbins, E. (2006) Membrane rafts in host-pathogen interactions. *Biochim. Biophys. Acta 1758*, 2139–2147.
8. Pucadyil, T. J., and Chattopadhyay, A. (2007) Cholesterol: A potential therapeutic target in *Leishmania* infection? *Trends Parasitol. 23*, 49–53.
9. Burger, K., Gimpl, G., and Fahrenholz, F. (2000) Regulation of receptor function by cholesterol. *Cell. Mol. Life Sci. 57*, 1577–1592.
10. Pucadyil, T. J., and Chattopadhyay, A. (2006) Role of cholesterol in the function and organization of G-protein coupled receptors. *Prog. Lipid Res. 45*, 295–333.
11. Paila, Y. D., and Chattopadhyay, A. (2010) Membrane cholesterol in the function and organization of G-protein coupled receptors. *Subcell. Biochem. 51*, 439–466.
12. Bloch, K. E. (1983) Sterol structure and membrane function. *CRC Crit. Rev. Biochem. 14*, 47–92.
13. Istvan, E. S., and Deisenhofer, J. (2002) Structural mechanism for statin inhibition of HMG-CoA reductase. *Science 292*, 1160–1164.
14. Menge, T., Hartung, H.-P., and Stüve, O. (2005) Statins: A cure-all for the brain? *Nat. Rev. Neurosci. 6*, 325–331.
15. Pierce, K. L., Premont, R. T., and Lefkowitz, R. J. (2002) Seven-transmembrane receptors. *Nat. Rev. Mol. Cell Biol. 3*, 639–650.
16. Rosenbaum, D. M., Rasmussen, S. G. F., and Kobilka, B. K. (2009) The structure and function of G-protein-coupled receptors. *Nature 459*, 356–363.
17. Pucadyil, T. J., Kalipatnapu, S., and Chattopadhyay, A. (2005) The serotonin$_{1A}$ receptor: A representative member of the serotonin receptor family. *Cell. Mol. Neurobiol. 25*, 553–580.
18. Gardier, A. M. (2009) Mutant mouse models and antidepressant drug research: Focus on serotonin and brain-derived neurotrophic factor. *Behav. Pharmacol. 20*, 18–32.
19. Pucadyil, T. J., and Chattopadhyay, A. (2004) Cholesterol modulates the ligand binding and G-protein coupling to serotonin$_{1A}$ receptors from bovine hippocampus. *Biochim. Biophys. Acta 1663*, 188–200.
20. Pucadyil, T. J., and Chattopadhyay, A. (2007) Cholesterol depletion induces dynamic confinement of the G-protein coupled serotonin$_{1A}$ receptor in the plasma membrane of living cells. *Biochim. Biophys. Acta 1768*, 655–668.
21. Zidovetzki, R., and Levitan, I. (2007) Use of cyclodextrins to manipulate plasma membrane cholesterol content: Evidence, misconceptions and control strategies. *Biochim. Biophys. Acta 1768*, 1311–1324.
22. Kalipatnapu, S., Pucadyil, T. J., Harikumar, K. G., and Chattopadhyay, A. (2004) Ligand binding characteristics of the human serotonin$_{1A}$ receptor heterologously expressed in CHO cells. *Biosci. Rep. 24*, 101–115.
23. Keyomarsi, K., Sandoval, L., Band, V., and Pardee, A. B. (1991) Synchronization of tumor and normal cells from G_1 to multiple cell cycles by lovastatin. *Cancer Res. 51*, 3602–3609.
24. Smith, P. K., Krohn, R. I., Hermanson, G. T., Mallia, A. K., Gartner, F. H., Provenzano, M. D., Fujimoto, E. K., Goeke, N. M., Olson, B. J., and Klenk, D. C. (1985) Measurement of protein using bicinchoninic acid. *Anal. Biochem. 150*, 76–85.
25. Amundson, D. M., and Zhou, M. (1999) Fluorometric method for the enzymatic determination of cholesterol. *J. Biochem. Biophys. Methods 38*, 43–52.
26. McClare, C. W. F. (1971) An accurate and convenient organic phosphorus assay. *Anal. Biochem. 39*, 527–530.
27. Higashijima, T., Ferguson, K. M., Sternweis, P. C., Smigel, M. D., and Gilman, A. G. (1987) Effects of Mg^{2+} and the $\beta\gamma$-subunit complex on the interactions of guanine nucleotides with G proteins. *J. Biol. Chem. 262*, 762–766.
28. Paila, Y. D., Murty, M. R. V. S., Vairamani, M., and Chattopadhyay, A. (2008) Signaling by the human serotonin$_{1A}$ receptor is impaired in cellular model of Smith-Lemli-Opitz Syndrome. *Biochim. Biophys. Acta 1778*, 1508–1516.
29. Lakowicz, J. R. (2006) Principles of Fluorescence Spectroscopy, 3rd ed., Springer, New York.
30. Umenishi, F., Verbavatz, J.-M., and Verkman, A. S. (2000) cAMP regulated membrane diffusion of a green fluorescent protein-aquaporin 2 chimera. *Biophys. J. 78*, 1024–1035.
31. Soumpasis, D. M. (1983) Theoretical analysis of fluorescence photobleaching recovery experiments. *Biophys. J. 41*, 95–97.
32. Radhakrishnan, A., Goldstein, J. L., McDonald, J. G., and Brown, M. S. (2008) Switch-like control of SREBP-2 transport triggered by small changes in ER cholesterol: A delicate balance. *Cell Metab. 8*, 512–521.
33. Mackinnon, W. B., May, G. L., and Mountford, C. E. (1992) Esterified cholesterol and triglyceride are present in plasma membranes of Chinese hamster ovary cells. *Eur. J. Biochem. 205*, 827–839.
34. Raymond, J. R., Olsen, C. L., and Gettys, T. W. (1993) Cell-specific physical and functional coupling of human 5-HT$_{1A}$ receptors to inhibitory G protein α-subunits and lack of coupling to Gsα. *Biochemistry 32*, 11064–11073.
35. Harikumar, K. G., and Chattopadhyay, A. (1999) Differential discrimination of G-protein coupling of serotonin$_{1A}$ receptors from bovine

hippocampus by an agonist and an antagonist. *FEBS Lett. 457*, 389–392.
36. Pucadyil, T. J., Kalipatnapu, S., Harikumar, K. G., Rangaraj, N., Karnik, S. S., and Chattopadhyay, A. (2004) G-protein-dependent cell surface dynamics of the human serotonin$_{1A}$ receptor tagged to yellow fluorescent protein. *Biochemistry 43*, 15852–15862.
37. Sinnecker, D., Voigt, P., Hellwig, N., and Schaefer, M. (2005) Reversible photobleaching of enhanced green fluorescent proteins. *Biochemistry 44*, 7085–7094.
38. Zhou, F. C., Patel, T. D., Swartz, D., Xu, Y., and Kelley, M. R. (1999) Production and characterization of an anti-serotonin$_{1A}$ receptor antibody which detects functional 5-HT$_{1A}$ binding sites. *Brain Res. Mol. Brain Res. 69*, 186–201.
39. Mukherjee, S., Kombrabail, M., Krishnamoorthy, G., and Chattopadhyay, A. (2007) Dynamics and heterogeneity of bovine hippocampal membranes: Role of cholesterol and proteins. *Biochim. Biophys. Acta 1768*, 2130–2144.
40. Vrljic, M., Nishimura, S. Y., Moerner, W. E., and McConnell, H. M. (2005) Cholesterol depletion suppresses the translational diffusion of class II major histocompatibility complex proteins in the plasma membrane. *Biophys. J. 88*, 334–347.
41. Nishimura, S. Y., Vrljic, M., Klein, L. O., McConnell, H. M., and Moerner, W. E. (2006) Cholesterol depletion induces solid-like regions in the plasma membrane. *Biophys. J. 90*, 927–938.
42. Lee, A. G. (2004) How lipids affect the activities of integral membrane proteins. *Biochim. Biophys. Acta 1666*, 62–87.
43. Palsdottir, H., and Hunte, C. (2004) Lipids in membrane protein structures. *Biochim. Biophys. Acta 1666*, 2–18.
44. Nyholm, T. K. M., Özdirekcan, S., and Killian, J. A. (2007) How protein transmembrane segments sense the lipid environment. *Biochemistry 46*, 1457–1465.
45. Opekarová, M., and Tanner, W. (2003) Specific lipid requirements of membrane proteins: A putative bottleneck in heterologous expression. *Biochim. Biophys. Acta 1610*, 11–22.
46. Chattopadhyay, A., and Paila, Y. D. (2007) Lipid-protein interactions, regulation and dysfunction of brain cholesterol. *Biochem. Biophys. Res. Commun. 354*, 627–633.
47. Porter, F. D. (2002) Malformation syndromes due to inborn errors of cholesterol synthesis. *J. Clin. Invest. 110*, 715–724.
48. Papakostas, G. I., Ongür, D., Iosifescu, D. V., Mischoulon, D., and Fava, M. (2004) Cholesterol in mood and anxiety disorders: Review of the literature and new hypotheses. *Eur. Neuropsychopharmacol. 14*, 135–142.
49. Paila, Y. D., and Chattopadhyay, A. (2009) The function of G-protein coupled receptors and membrane cholesterol: Specific or general interaction? *Glycoconjugate J. 26*, 711–720.
50. Paila, Y. D., Tiwari, S., and Chattopadhyay, A. (2009) Are specific nonannular cholesterol binding sites present in G-protein coupled receptors? *Biochim. Biophys. Acta 1788*, 295–302.
51. Hanson, M. A., Cherezov, V., Griffith, M. T., Roth, C. B., Jaakola, V.-P., Chien, E. Y. T., Velasquez, J., Kuhn, P., and Stevens, R. C. (2008) A specific cholesterol binding site is established by the 2.8 Å structure of the human β_2-adrenergic receptor. *Structure 16*, 897–905.
52. Kenworthy, A. K., Nichols, B. J., Remmert, C. L., Hendrix, G. M., Kumar, M., Zimmerberg, J., and Lippincott-Schwartz, J. (2004) Dynamics of putative raft-associated proteins at the cell surface. *J. Cell Biol. 165*, 735–746.
53. Bacia, K., Scherfeld, D., Kahya, N., and Schwille, P. (2004) Fluorescence correlation spectroscopy relates rafts in model and native membranes. *Biophys. J. 87*, 1034–1043.
54. Adkins, E. M., Samuvel, D. J., Fog, J. U., Eriksen, J., Jayanthi, L. D., Vaegter, C. B., Ramamoorthy, S., and Gether, U. (2007) Membrane mobility and microdomain association of the dopamine transporter studied with fluorescence correlation spectroscopy and fluorescence recovery after photobleaching. *Biochemistry 46*, 10484–10497.
55. Pralle, A., Keller, P., Florin, E.-L., Simons, K., and Hörber, J. K. H. (2000) Sphingolipid-cholesterol rafts diffuse as small entities in the plasma membrane of mammalian cells. *J. Cell Biol. 148*, 997–1007.
56. Kwik, J., Boyle, S., Fooksman, D., Margolis, L., Sheetz, M. P., and Edidin, M. (2003) Membrane cholesterol, lateral mobility, and the phosphatidylinositol 4,5-bisphosphate-dependent organization of cell actin. *Proc. Natl. Acad. Sci. U.S.A. 100*, 13964–13969.
57. Ganguly, S., Pucadyil, T. J., and Chattopadhyay, A. (2008) Actin cytoskeleton-dependent dynamics of the human serotonin$_{1A}$ receptor correlates with receptor signaling. *Biophys. J. 95*, 451–463.
58. Ikonen, E. (2008) Cellular cholesterol trafficking and compartmentalization. *Nat. Rev. Mol. Cell Biol. 9*, 125–138.
59. Endo, A. (1992) The discovery and development of HMG-CoA reductase inhibitors. *J. Lipid Res. 33*, 1569–1582.
60. Golomb, B. A., Criqui, M. H., White, H., and Dimsdale, J. E. (2004) Conceptual foundations of the UCSD statin study: A randomized controlled trial assessing the impact of statins on cognition, behavior, and biochemistry. *Arch. Intern. Med. 164*, 153–162.
61. Mauch, D. H., Nägler, K., Schumacher, S., Göritz, C., Müller, E.-C., Otto, A., and Pfrieger, F. W. (2001) CNS synaptogenesis promoted by glia-derived cholesterol. *Science 294*, 1354–1357.
62. Dietschy, J. M., and Turley, S. D. (2001) Cholesterol metabolism in the brain. *Curr. Opin. Lipidol. 12*, 105–112.
63. Vance, J. E., Hayashi, H., and Karten, B. (2005) Cholesterol homeostasis in neurons and glial cells. *Semin. Cell Dev. Biol. 16*, 192–212.
64. Porter, F. D. (2008) Smith-Lemli-Opitz syndrome: Pathogenesis, diagnosis and management. *Eur. J. Hum. Genet. 16*, 535–541.
65. Beasley, C. L., Honer, W. G., Bergmann, K., Falkai, P., Lütjohann, D., and Bayer, T. A. (2005) Reductions in cholesterol and synaptic markers in association cortex in mood disorders. *Bipolar Disord. 7*, 449–455.
66. Kirsch, C., Eckert, G. P., and Mueller, W. E. (2003) Statin effects on cholesterol micro-domains in brain plasma membranes. *Biochem. Pharmacol. 65*, 843–856.
67. Green, R. C., McNagny, S. E., Jayakumar, P., Cupples, L. A., Benke, K., and Farrer, L. A. (2006) Statin use and the risk of Alzheimer's disease: The MIRAGE study. *Alzheimers Dementia 2*, 96–103.